AUGUST 1978 PPPL-1470
UC-20g

DEPENDENCE OF IDEAL MHD KINK AND BALLOONING MODES ON PLASMA SHAPE AND PROFILES IN TOKAMAKS

PLASMA PHYSICS LABORATORY

PRINCETON UNIVERSITY
PRINCETON, NEW JERSEY

This work was supported by the U. S. Department of Energy Contract No. EY-76-C-02-3073. Reproduction, translation, publication, use and disposal, in whole or in part, by or for the United States Government is permitted.

Dependence of Ideal MHD Kink and Ballooning Modes on Plasma Shape and Profiles in Tokamaks

A. M. M. Todd, J. Manickam, M. Okabayashi, M. S. Chance, R. C. Grimm, J. M. Greene, and J. L. Johnson*
Princeton University Plasma Physics Laboratory
Princeton, New Jersey 08540

ABSTRACT

Extensive numerical studies of ideal MHD instabilities have been carried out to gain insight into the parametric dependence of critical β's in tokamaks. The large number of interrelated equilibrium quantities involved in establishing a critical β has demanded a careful, systematic survey in order to isolate this dependence. The results of this survey establish the scaling with geometrical quantities including aspect ratio, elongation, and triangularity in the parameter regimes appropriate for both current and reactor-sized plasmas. A moderate dependence on the pressure profile and a strong variation with the current profile is found. The principal result is that for aspect ratio R/a ≥ 3, critical β's are of the order of 2% for circular cross sections and 5% for plasmas with elongation $\kappa \simeq 2$; somewhat higher values could be achieved with more optimal shaping. Finally, sequences of equilibria have been analyzed to compare critical β as a function of toroidal mode number n. We conclude that the infinite-n analytic ballooning theory provides a sufficient condition for ideal MHD internal mode stability. Low-n free boundary modes appear to set a lower limit.

I. INTRODUCTION

The practical feasibility of tokamaks as fusion reactors will depend strongly on the density and pressure of the confined plasma. Given the technological limitations on the achievable field strength with superconducting magnets, it is therefore desirable to maximize β, the ratio of material to magnetic pressure in the plasma. There are many physical effects which influence this maximum β. Perhaps the simplest and most straightforward limit is set by the ideal MHD linear stability of the plasma configuration to pressure and current driven modes. Of course, this value may be pessimistic since for example, nonlinear saturation of the modes above the marginal β may occur. On the other hand, the inclusion of resistive behavior should lead to a lower limit by allowing the interchange of field and plasma and introducing the possibility of tearing modes. Nevertheless, ideal linear stability has always provided a useful guideline to the achievable plasma β.

The complex interdependence of the plasma equilibrium parameters at moderate β values and their strong effect on stability renders general analysis difficult. Consequently, using the Princeton Equilibrium, Stability, and Transport Code (PEST) [1], we have performed a computational survey in which we vary only a single element in parameter space at a time. Our results are not restricted to a particular tokamak device and do not determine absolute values of the achievable β. They do, however, demonstrate trends and

complement the intuition obtained from analytic studies to substantiate our understanding of the physical effects involved. Hopefully, this work indicates the direction that should be pursued in experimental devices where current technology does not permit subtle manipulation of the plasma profiles.

In Section II we identify the instabilities of interest and discuss the parameter space that is investigated. In Section III we describe the computational techniques used to obtain the critical β's and define our equilibrium model. In Section IV we present the results of the survey. In Section V we give our interpretation of the results and present some conclusions.

II. INSTABILITIES OF INTEREST

Ideal MHD stability considerations have shown that the free surface current and pressure driven modes are likely to limit β. Of these, the axisymmetric instabilities with toroidal mode number n = 0 are potentially dangerous, especially for systems with a noncircular plasma cross section [2]. Since it has been shown that this mode can be controlled with a passive feedback system [3], it will not be discussed in this paper.

The n = 1 kink mode, driven largely by force-free currents along the magnetic field lines is very limiting and must form the heart of any investigation.

It is generally expected that this mode can be controlled by locally shaping the force-free current or by external feedback. Therefore, it is useful also to consider β limitations associated with internal modes where the plasma surface is held fixed. Of these, modes with relatively low values of n, driven mainly by pressure gradients in regions of unfavorable curvature, seem important since their eigenfunctions show deep convective channels that extend from near the magnetic axis to the plasma boundary. We have concentrated on the $n = 3$ mode for our numerical studies because this n is large enough that the mode is primarily pressure driven and yet small enough that the mode is adequately represented numerically.

As $n \to \infty$ it is possible to use an analytic treatment, obtained in the limit where derivatives normal to the magnetic surfaces, while large when compared to those along the field $\underset{\sim}{B}$, are much smaller than those in the $\underset{\sim}{B} \times \nabla V$ direction [4, 5]. Then the modes on the different magnetic surfaces decouple to lowest order in an expansion in $1/n$, and stability can be studied by solving the ordinary differential equation on each magnetic surface

$$\frac{\partial}{\partial\theta}\left\{\frac{4\pi^2q^2}{X^2B^2}\left[\frac{1}{X^2q^2}+\left(\frac{q'}{q}\right)^2\theta^2|\underset{\sim}{\nabla}\psi|^2+2\left(\frac{q'}{q}\right)\theta\underset{\sim}{\nabla}\psi\cdot\underset{\sim}{\nabla}\theta+|\underset{\sim}{\nabla}\theta|^2\right]\frac{\partial F}{\partial\theta}\right\}$$

$$+\frac{p'X^2}{R^2}\left[\frac{p'}{B^2}+\frac{q'}{q}+\left(\frac{q'}{q}\right)\left(\frac{R^2q^2}{X^2B^2}-1\right)-2\frac{X'}{X}-\frac{1}{4\pi^2X^2}\frac{\partial}{\partial\theta}\left(\frac{\underset{\sim}{\nabla}\psi\cdot\underset{\sim}{\nabla}\theta}{B^2}\right)\right.$$

$$\left.-\frac{R^2q^2}{X^2B^4}\left(\frac{q'}{q}\right)\theta\frac{\partial B^2}{\partial\theta}\right]F=0\ . \qquad (1)$$

Here we have adopted the notation of the PEST code [1]: X is the distance from the axis of symmetry, R is the location of the magnetic axis, q is a stream function for the toroidal field, q is the safety factor, primes denote derivatives with respect to the poloidal flux ψ, and the dependent variable F is related to the normal displacement ξ_ψ.

Thus, we determine critical β's primarily for the n = 1 free surface kink mode, the n = 3 internal ballooning mode, and the $n \to \infty$ internal ballooning mode. For typical tokamak operating conditions the Mercier criterion for localized stability is usually met. In all configurations reported here this condition is satisfied.

We divide our discussion of parameter studies into three broad groups. In the first we consider purely geometric

parameters. These include the aspect ratio and the shape of the cross section. We define the shape in terms of ellipticity and triangularity parameters that determine the plasma boundary. Our second group treats the variation of the internal plasma properties associated with the current in the plasma, determined by the safety factor $q(\Psi)$ and the pressure $p(\Psi)$ profiles. Our third group consists of varying the external conditions as reflected in the boundary conditions for the instabilities. Thus we treat systems where the plasma has a vacuum region between a free boundary surface and a perfectly conducting wall at infinity or at a finite distance. We also hold the plasma surface fixed and look at internal modes. We then consider the effect of adding a perfectly conducting plasma which is pressureless but can support force-free current perturbations outside the main body of the plasma. Finally, we consider the critical for stability of a specific system as a function of the toroidal mode number n in order to show the importance of the different modes.

III. COMPUTATIONAL PROCEDURE AND EQUILIBRIUM MODEL

We use a systematic procedure to study the variation of the critical β with any given parameter. We obtain an initial equilibrium with the appropriate parameters and then generate a series of flux-conserved equilibria with the same boundary shape,

q-profile and shape of pressure profile but with increasing β [6]. The generation of such sequences requires the adjustment of the currents in the external coils and the use of the PEST equilibrium code procedure [7].

We use the PEST code [1] to determine the stability of these equilibrium series, employing the same techniques that were used previously [8]. Thus, we do not solve explicitly for the marginal point β_c, but extrapolate to obtain the critical β from a set of values of the growth rate versus β for $\beta > \beta_c$. Each of these growth rates is itself obtained by extrapolation to the limit from a set of distinct numerical calculations with an increasing number of expansion functions [9].

The shape of the plasma boundary, shown in Fig. 1, is given by

$$X = X_0 + a \cos(\theta + \delta \sin\theta) , \tag{2}$$

$$Z = K a \sin\theta , \tag{3}$$

where X increases outward from the axis of symmetry and Z along that axis, X_0 is the position of the center of the surface, a is the mirror radius, K and δ are parameters that measure the ellipticity and triangularity, and θ is an angle around a center at $X = X_0$, $Z = 0$. A value of $\delta = 0.5$ corresponds to a strongly D-shaped plasma; $\delta = 0.25$ gives weak triangularity.

The pressure is given by

$$p(\Psi) = p_o \left(\frac{\Psi_b - \Psi}{\Psi_b - \Psi_a} \right)^{\alpha} \tag{4}$$

with Ψ_b and Ψ_a the poloidal flux at the plasma boundary and at the magnetic axis respectively. The parameter α allows for considerable choice in the shape of the distribution. Thus, $\alpha = 1$ corresponds to a broad profile while $\alpha = 2$ yields a fairly peaked one. With $\alpha > 1$ there is no current at the plasma-vacuum interface associated with pressure gradients. The parameter p_o is adjusted to give the desired value of β.

We use the safety factor q, a surface function, to specify the shape of the force-free current distribution. For most of our studies q increases monotonically from just above one at the magnetic axis to 3.8 at the boundary, as in Fig. 2. In our investigation of the effect of changing the current distribution we have changed q at the boundary, q_b, keeping q at the axis, q_a, fixed and q_a keeping q_b fixed.

In generating the sequences of equilibria needed for these studies we take advantage of the similarity scaling law noted by Bateman and Peng [10]. Thus if we scale $p \to s^2 p$ and $\Psi \to s\Psi$, then q scales approximately as q/s. To obtain two sequences of flux-conserved-tokamak equilibria with different q_a but identical q_b, we begin with any two sequences which differ only in their

q profiles, say, $q_a^{(1)}$, $q_b^{(1)}$ and $q_a^{(2)}$, $q_b^{(2)}$. The value of s which scales $q_b^{(2)}$ to $q_b^{(1)}$ is then used to scale each member of the second sequence to the desired family. The critical β of this second sequence is obtained in the usual way. The advantage of the scaling law is, of course, that by applying it also to $q_a^{(2)}$ we can trivially generate a third sequence with varying q_b but identical q_a to the first. The application of this process to three sequences is illustrated in Fig. 2, which shows the q profiles used in the studies for Figs. 7 and 8. We remark in passing that the critical β's obtained from this procedure are, of course, not at constant β_0 or total current.

In our studies of the effects of boundary conditions, the external modes are usually treated with the conducting wall infinitely far from the plasma and the currents in the external coils unaffected by the perturbations (infinite impedance). We also study the effect of having a conducting shell at a uniform distance outside the plasma with the same shape as the boundary. Additionally, we treat the situation where the region between r_b and an outer surface is filled with a pressureless plasma. The strongest stabilizing external constraint is to hold the plasma surface fixed.

In any attempt to optimize parameters, it is useful to note that the amount of fusion energy obtained will vary as p^2. Thus it is most reasonable to define β as

$$\beta = 2\mu_o \left(\int p^2 \, dV/V \right)^{1/2} B_o^{-2} \qquad (5)$$

as we do for the purposes of this study. This leads to more optimistic numbers, by a factor of 1.3 to 1.5, than one would get with the usual definition using the average pressure.

IV. RESULTS

The dependence of β_c on the aspect ratio is simple and predictable. As shown in Fig. 3, it is linear in a/R for systems with both circular and noncircular cross sections. In both cases the pressure profile is given by $\alpha = 2$ and the safety factor q goes from 1 on axis to 3.8 at the plasma edge. In the noncircular case the ellipticity $K = 1.65$ and the triangularity $\delta = 0.25$. For both cases we give results for the $n = 1$ and $n = 3$ free surface kink modes and the $n = 3$ fixed boundary internal ballooning mode.

Figure 4 shows the dependence of the critical β on elongation. In making this study we use a D-shaped plasma since some triangularity is needed to preserve Mercier stability in elongated systems. We set $R/a = 3.0$, $\delta = 0.25$, $\alpha = 2.0$, and $1.0 < q < 3.8$ and observe a moderate increase in β_c with K for the $n = 1$ and $n = 3$ modes with a free surface, the $n = 3$ fixed boundary mode, and the $n \to \infty$ ballooning mode. It is interesting

to note that the $n \to \infty$ results are quite close to those for free boundary modes. This study indicates that there is a maximum ellipticity above which little further gain is achieved.

Triangularity is helpful only for systems with noncircular cross sections. To study its effect we set R/a = 3.0, K = 1.65, $1.0 < q < 3.8$, and $\alpha = 2$. Figure 5 gives the dependence of β_c on δ. We note that small triangularity does not provide significant improvement over the purely elliptical case. Only modest gain is achieved with $\delta = 0.5$. Again, the $n \to \infty$ ballooning results differ little from the n = 1 free surface ones.

To study the effect of changing the pressure profile we take equilibria with R/a = 3.5, K = 1.65, $\delta = 0.25$, $1.0 < q < 3.0$ and vary the exponent α in Eq. (4) between 1.2 and 2.0. The results are given in Fig. 6. Making the profile flatter by decreasing α improves the stability of the internal modes. This is not surprising since as α is decreased the destabilization region is pushed more and more towards the outside where the plasma is held fixed.

Although reducing the current gradient near the plasma vacuum interface is usually considered to improve external kink mode stability [11], this effect is only obvious at low β. As seen here at higher β, even the low n external modes have a considerable internal ballooning component which can be stabilized in the plasma interior by adjusting the pressure profile as noted for pure internal modes. As α is decreased, the destabilization region is moved to the edge of the plasma where for D-shaped plasmas there is increasing shear due to the nearness of the separatrix surface.

We have used the two families of q profiles of Fig. 2 to study the effect of changing the current shape. The results of changing q_b, keeping q_a fixed at 1.0, are shown in Fig. 7 where we have considered a system with R/a = 4.6, K = 1.0, δ = 0.0, and α = 1.4. Surprisingly different results were obtained for a case with R/a = 4.6, K = 1.0, δ = 0.0, and α = 2 when we changed q_a keeping q_b fixed at 3.8 as can be seen in Fig. 8. The critical β for internal modes starts to decrease with q_a but then increases such that when $q_a \approx 2.5$, $\beta_c \approx 2\%$. A dramatic improvement in the critical β for the $n \to \infty$ ballooning mode is also observed. In both cases though the critical β for the free boundary n = 1 mode is lowered by decreasing shear as one would expect.

We turn now to the effect of changing the external conditions. In Fig. 9 we plot unconverged data showing the growth rate of the n = 3 mode, normalized to the poloidal Alfvén frequency at the plasma boundary as a function of β for different positions of a perfectly conducting wall shaped like the interface for a case with R/a = 3.5, K = 1.65, δ = 0.25, α = 1.4, and 1.0 < q < 3.0. Here a and b represent the respective half widths of the plasma and the wall. We note that the transition from an external kink to an internal ballooning mode is obtained even with the wall at a considerable distance from the plasma. It is useful to examine the eigenfunctions, shown in Figs. 10 - 13, to see the transition from external to internal variation.

We use this same equilibrium, $R/a = 3.5$, $K = 1.65$, $\delta = 0.25$, $\alpha = 1.4$, $1 \leq q \leq 3.0$ to study the effect of introducing a pressureless plasma in the vacuum region. In this case we treat the region between the current-carrying column bounded by the $q = 3$ surface and a magnetic surface with safety factor q_e as perfectly conducting, but with no equilibrium pressure or current, and the region outside this surface as a vacuum. In Fig. 14 we plot the unconverged growth rate of the $n = 1$ mode as a function of q_e. The growth rate plotted here is normalized to the case where $q_e = 3$; i.e., without any pressureless plasma. We assume a constant density out to the edge of the pressureless plasma, but keep the total mass in the system fixed.

Finally, we show in Figs. 15 and 16 critical β as a function of $1/n$ for both free surface and fixed boundary modes. Clearly the low n free boundary kinks provide the most severe restrictions. It is useful to note the good correlation between the predictions of the $n \to \infty$ model, carried to lowest order in an expansion in $1/n$, and the numerical results.

V. INTERPRETATION AND CONCLUSIONS

The results from the PEST code substantiate our intuitive understanding of the effects of changing the geometrical properties of the system. In particular, the destabilization

associated with pressure gradients in a curved magnetic field is proportional to the curvature of the toroidal component of the field and thus scales as a/R in a tokamak. Similarly, the force-free current that drives kink modes also scales as a/R for fixed q. Thus a linear dependence on this parameter, as is seen in Fig. 3 should be expected.

Turning to the elongation and triangularity, it appears that the main effect of increasing these is to modify the local pitch of the magnetic field lines so as to shorten the connection length. As can be seen from Figs. 4 and 5, there is a tendency for this effect to saturate for the n = 3 modes. At large ellipticities, the separatrix comes close to the plasma and we have difficulty obtaining equilibria with the q profile exactly conserved. The improvement of the n = 1 mode should also level off if q is held constant. These modes also saturate with δ. This is probably due to the fact that improvement of the connection length is limited.

We saw considerable improvement when we changed the shape of the pressure distribution in Fig. 6 for the internal modes. The internal modes are more stable for broader profiles where the pressure gradient occurs mainly near the fixed plasma edge. Similar results have been found by Wesson [11]. The variation in critical β with α for the external modes was less significant.

The interpretation of the results of changing the safety factor profile, shown in Figs. 7 and 8, is less straightforward. In general, the external modes are strongly destabilized by decreasing the shear while the internal modes are stabilized by decreasing the magnitude of q. This behavior seems to be reasonable: The decrease of q and q' is associated with an increase of the force-free current that drives kink modes as well as a decrease in the shear stabilization that could be expected. On the other hand, decreasing q shortens the connection length, raising the critical β for internal ballooning modes. The improvement in critical β for internal modes observed when q_a is increased keeping q_b fixed, thereby reducing the shear, which was also seen by Sykes et al. [12], furnishes a dramatic departure from this intuition. In addition to the PEST studies, it is found with the $n \to \infty$ balloon model. A probable explanation can be seen by considering Eq. (1). For the high-n modes the most significant place that q' enters is the coupling of the destabilizing geodesic curvature term [the last term in Eq. (1)] at large θ. Thus the observed behavior of the n = 3 internal mode can be explained as follows. Initially, as q_a is increased from unity, the increase in connection length destabilizes the plasma. Eventually however, the improvement of the average minimum B of the system and the reduction of the coupling of the mode to the geodesic curvature overcomes the increase in connection length, so that the plasma becomes increasingly stable. Mercier [13] has observed a high-β stabilization related to this

effect of decreasing the effective field curvature destabilization. We have analyzed a series of equilibria generated with the current profiles of Sykes et al., [12] showing that this decoupling of the geodesic curvature is responsible for their observed internal mode stability at high β. Unfortunately, it is unlikely that the plasma could support profiles with such high q_a's over many transport times.

The interesting result, Fig. 9, of placing a conducting shell outside the plasma was the significant stabilization achieved even with the wall at a significant distance from the plasma. Since these external modes tend to be localized primarily on the outside near the regions of bad curvature as can be seen in Fig. 10, one conjectures that the same effect could be achieved by placing a conducting plate or limiter there. Further study of the effect of different wall shapes or of boundary condition modification due to individual coils would be useful.

The rapid improvment in growth rate as a region of currentless conducting plasma is introduced outside the plasma reflects both improvements due to more optimal shaping of the current and its derivatives near the plasma edge and the constraints imposed by including additional rational surfaces in the plasma region. The step structure located near rational q_e demonstrates this latter phenomenon. Coupling of the various Fourier modes by noncircularity and toroidicity is no doubt responsible for smoothing this step structure out. The fact that one must introduce a large region before achieving stability must serve as a

warning that stabilization of external modes by current shaping will not be easy or automatic.

Possibly the most interesting part of the survey concerns the relation between modes with different mode numbers n exhibited in Figs. 15 and 16. Clearly for these equilibrium sequences, the $n \to \infty$ limit provides the most severe limit for internal modes. In fact, based on a considerable experience with other sequences, our evidence suggests this to be a general rule. For cases that have been examined keeping 1/n corrections [14], the predictions of this theory are in good agreement with the results of PEST for internal modes with n = 3 or 5. Detailed study of free boundary modes is still necessary.

In this study we have not attempted to find the maximum β achievable within the confines of the model. We have tried to clarify the physical dependence of these ideal MHD modes on specific parameters. This should enable us to guide experiments towards regimes where the instabilities should occur--these are substantially above any present tokamak operating regime where $\beta \geq 1\%$ has not been achieved. The actual behavior of these instabilities should be examined to determine their real danger. In particular, it is essential to determine the actual threat posed by free boundary kink modes since, as has been shown, these modes onset at the lowest β values, are critically dependent on boundary conditions, and in general have the opposite dependence on profile shaping to that of internal ballooning modes.

ACKNOWLEDGMENTS

We gratefully acknowledge the programming assistance of Dr. Y. Y. Hsieh. We are indebted to Dr. R. A. Dory for suggesting the equilibrium shape used in this study. We appreciate the help and suggestions of our colleagues at the Plasma Physics Laboratory. In particular the prodding and guidance provided by P. H. Rutherford was most useful.

This work was supported by United States Department of Energy Contract No. EY-76-C-02-3073.

REFERENCES

* On loan from Westinghouse Research and Development Center.

[1] GRIMM, R. C., GREENE, J. M., and JOHNSON, J. L., in Methods in Computational Physics, Vol. 16, ed. Killeen, J. (Academic Press, New York, 1976), p. 253.

[2] JOHNSON, J. L., CHANCE, M. S., GREENE, J. M., GRIMM, R. C., JARDIN, S. C., KERNER, W., MANICKAM, J., and WEIMER, K. E., in Plasma Physics and Controlled Nuclear Fusion Resear 1976, (International Atomic Energy Agency, Vienna, 1977) Vol. 1, p. 395.

[3] JARDIN, S. C., Phys. Fluids (in preparation).

[4] DOBROTT, D., NELSON, D. B., GREENE, J. M., GLASSER, A. H., CHANCE, M. S., and FRIEMAN, E. A., Phys. Rev. Lett. 39 (1977) 943.

[5] CONNOR, J. W., HASTIE, R. J., and TAYLOR, J. B., Phys. Rev. Lett. 40 (1978) 396.

[6] DORY, R. A. and PENG, Y.-K. M., Nucl. Fusion 17 (1977) 21.

[7] JOHNSON, J. L., DALHED, H. E., GREENE, J. M., GRIMM, R. C., HSEIH, Y. Y., JARDIN, S. C., MANICKAM, J., OKABAYASHI, M., STORER, R. G., TODD, A. M. M., VOSS, D. E., and WEIMER, K. E. (submitted to J. Comput. Phys.).

[8] TODD, A. M. M., CHANCE, M. S., GREENE, J. M., GRIMM, R. C., JOHNSON, J. L., and MANICKAM, J., Phys. Rev. Lett. 38 (1977) 826.

[9] CHANCE, M. S., GREENE, J. M., GRIMM, R. C., JOHNSON, J. L., MANICKAM, J., KERNER, W., BERGER, D., BERNARD, L. C., GRUBER, R., and TROYON, F., J. Comput. Phys. (in press).

[10] BATEMAN, G. and PENG, Y.-K. M., Phys. Rev. Lett, 38 (1977) 829.

[11] WESSON, J. A., Nucl. Fusion 18 (1978) 87.

[12] SYKES, A., WESSON, J. A., and COX, S. J., Phys. Rev. Lett. 39 (1977) 757.

[13] MERCIER, C., in Seventh Conference on Plasma Physics and Controlled Nuclear Fusion Reactions, Innsbruck (1978).

[14] FRIEMAN, E. A., MANICKAM, J., CHANCE, M. S., DEWAR. R. L., GLASSER, A. H., GREENE, J. M., GRIMM, R. C., JARDIN, S. C., JOHNSON, J. L., OKABAYASHI, M., and TODD, A. M. M., in Seventh Conference on Plasma Physics and Controlled Nuclear Fusion Reactions, Innsbruck (1978).

FIGURE CAPTIONS

Fig. 1. Geometry of comparison model. The inner surface is the plasma surface given by $X = X_o + a\cos(\theta + \delta \sin\theta)$, $Z = K a \sin\theta$, with $A = X_o/a$ the aspect ratio, K a measure of the elongation, and δ the triangularity parameter. The outer surface, a fixed distance $b - a$ out from the plasma along rays from X_o, forms a perfectly conducting wall.

Fig. 2. Safety factor q as a function of the poloidal flux $\bar{\Psi} = (\Psi - \Psi_a)/(\Psi_b - \Psi_a)$ for the current distributions considered in this paper.

Fig. 3. Critical $\beta \equiv 2\mu_o \left(\int p^2 \, dV/V \right)^{1/2} B_o^{-2}$ as a function of the inverse aspect ratio for configurations with a D-shape cross section, $K = 1.65$, $\delta = 0.25$ (upper curves), and a circular cross section, $K = 1.0$, $\delta = 0.0$ (lower curves); $\alpha = 2.0$, $1.0 < q < 3.8$. The circles denote $n = 1$ free boundary modes, squares correspond to $n = 3$ free boundary modes and triangles represent $n = 3$ modes with the plasma surface held fixed.

Fig. 4. Critical β as a function of ellipticity for a configuration with $A = 3.0$, $\delta = 0.25$, $\alpha = 2.0$, and $1 < q < 3.8$. Solid points represent the $n \to \infty$ ballooning code results.

Fig. 5. Critical β as a function of triangularity for a configuration with $A = 3.0$, $K = 1.65$, $\alpha = 2$, and $1 < q < 3.8$.

Fig. 6. Critical β as a function of the pressure distribution parameter α. The shapes of $p(\Psi)$ are shown in the inset for $\alpha = 1.2$ and $\alpha = 2.0$.

Fig. 7. Critical β as a function of q_b with q_a fixed at 1.0 for a configuration with $A = 4.6$, $K = 1.0$, $\delta = 0.0$, $\alpha = 2$, and the distributions of Fig. 2.

Fig. 8. Critical β as a function of q_a with q_b fixed at 3.8 for the configuration of Fig. 7.

Fig. 9. Growth rate, normalized to the shear Alfvén time at the plasma edge, as a function of β for a conducting wall at $b/a = \infty$, 1.7, 1.3, and 1.0; $A = 3.5$, $K = 1.65$, $\delta = 0.25$, $\alpha = 1.4$, $1 < q < 3.0$, and $n = 3$.

Fig. 10. Projection of the displacement vector of the $n = 3$ free boundary ($b/a = \infty$) mode for the configuration of Fig. 9.

Fig. 11. Radial dependence of different Fourier components of ξ_ψ along the $\theta = 0$ axis for the displacement vector of Fig. 10.

Fig. 12. Projection of the displacement vector of the $n = 3$, fixed boundary ($b/a = 1$) mode for the configuration of Fig. 9.

Fig. 13. Radial dependence of different Fourier components of ξ_ψ along the $\theta = 0$ axis for the displacement vector of Fig. 12.

Fig. 14. Unconverged growth rate as a function of the value of q at the edge of a pressureless plasma region for a configuration with $A = 3.5$, $K = 1.65$, $\delta = 0.25$, $\alpha = 1.4$, $1 < q < 3$ inside the plasma, and $\beta = 7.3\%$.

Fig. 15. Critical β as a function of $1/n$ for a configuration with $R/a = 3.5$, $K = 1.65$, $\delta = 0.25$, $\alpha = 1.4$, and $1.0 < q < 3.0$.

Fig. 16. Critical β as a function of $1/n$ for a configuration with $R/a = 4.6$, $K = 1.0$, $\delta = 0$, $\alpha = 2$, and $1.04 < q < 1.58$.

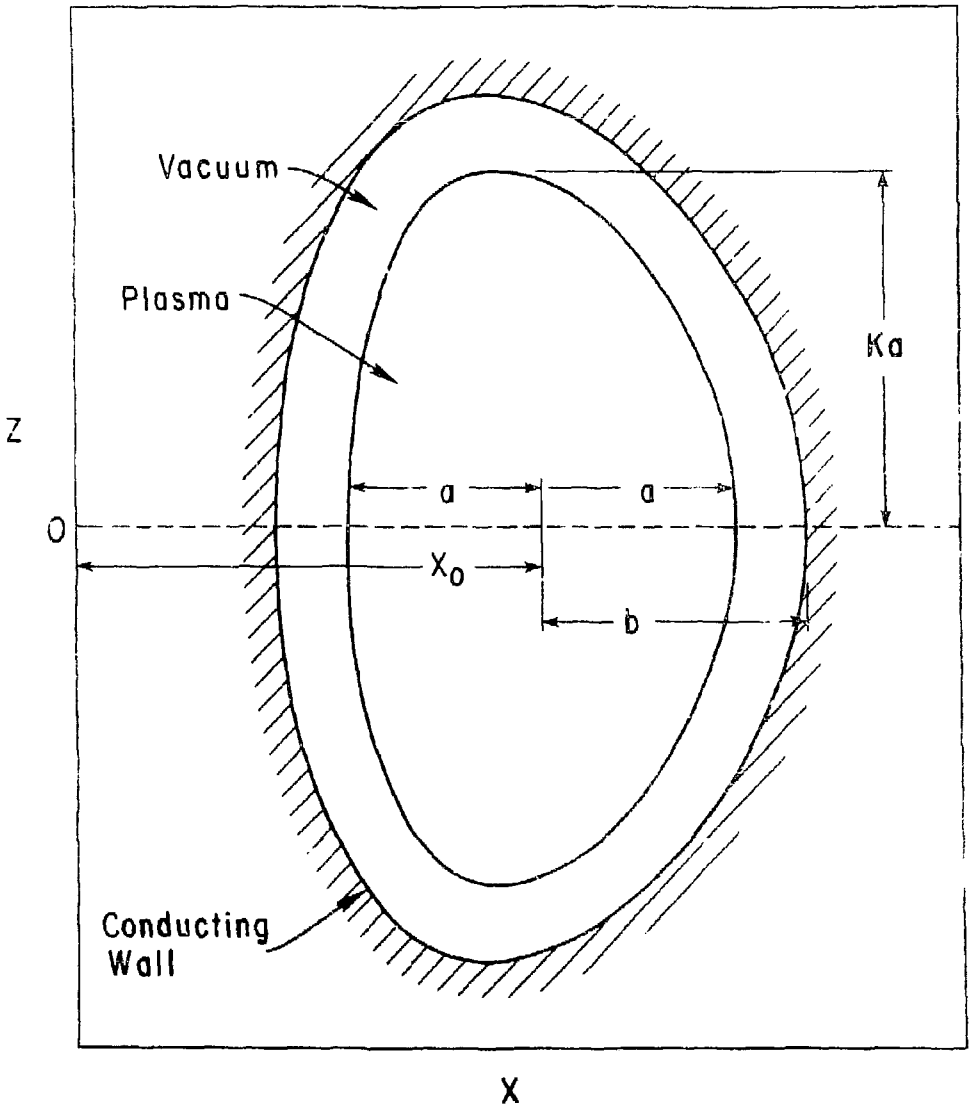

Fig. 1. 782225

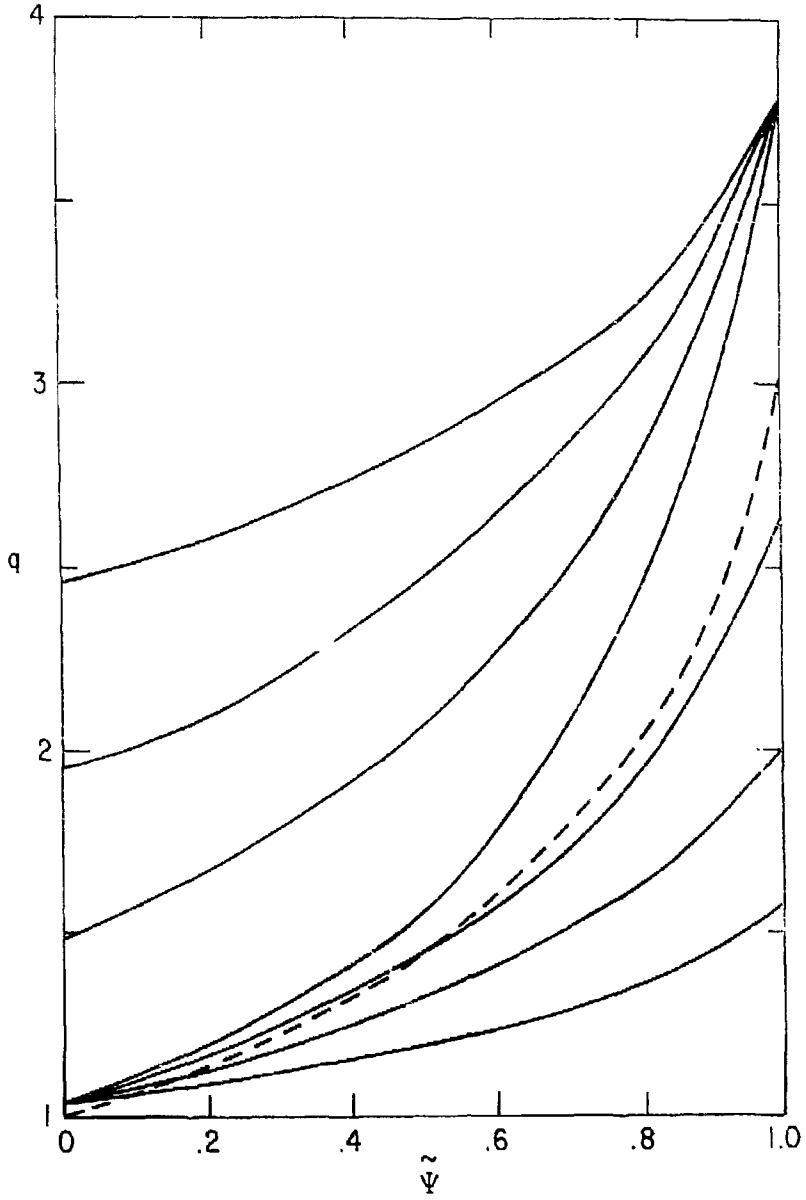

Fig. 2. 782247

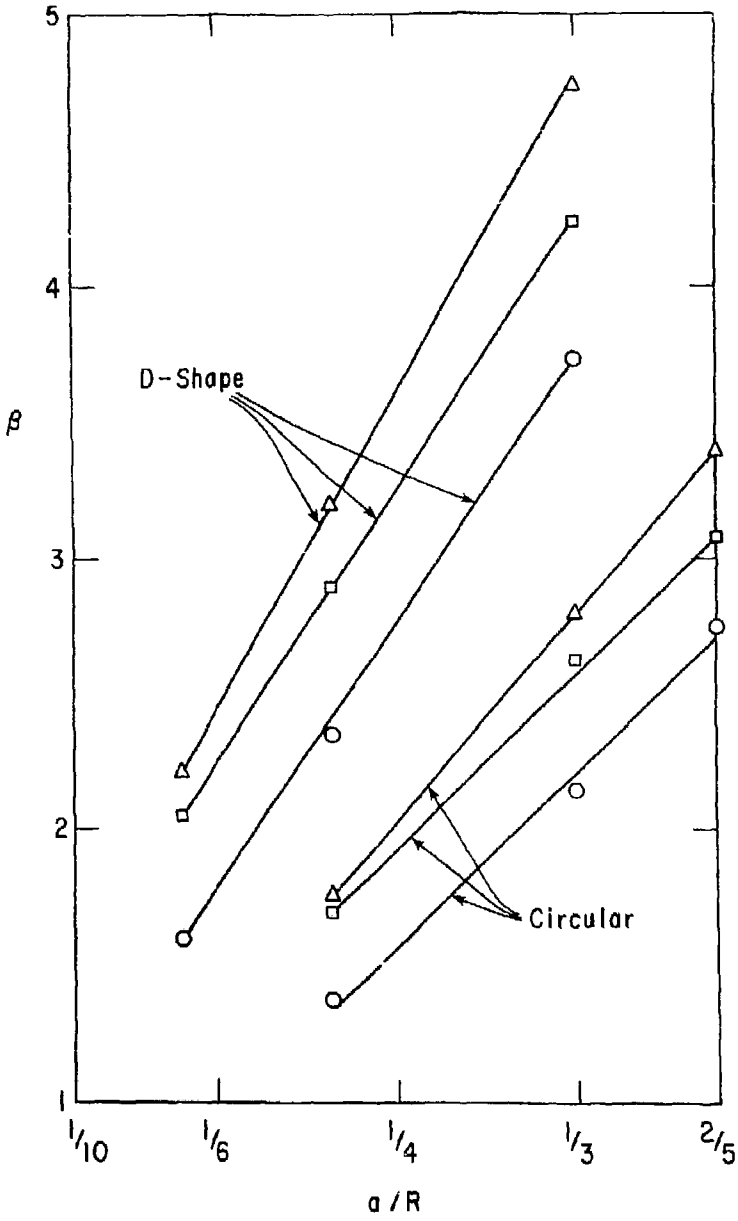

Fig. 3. 782228

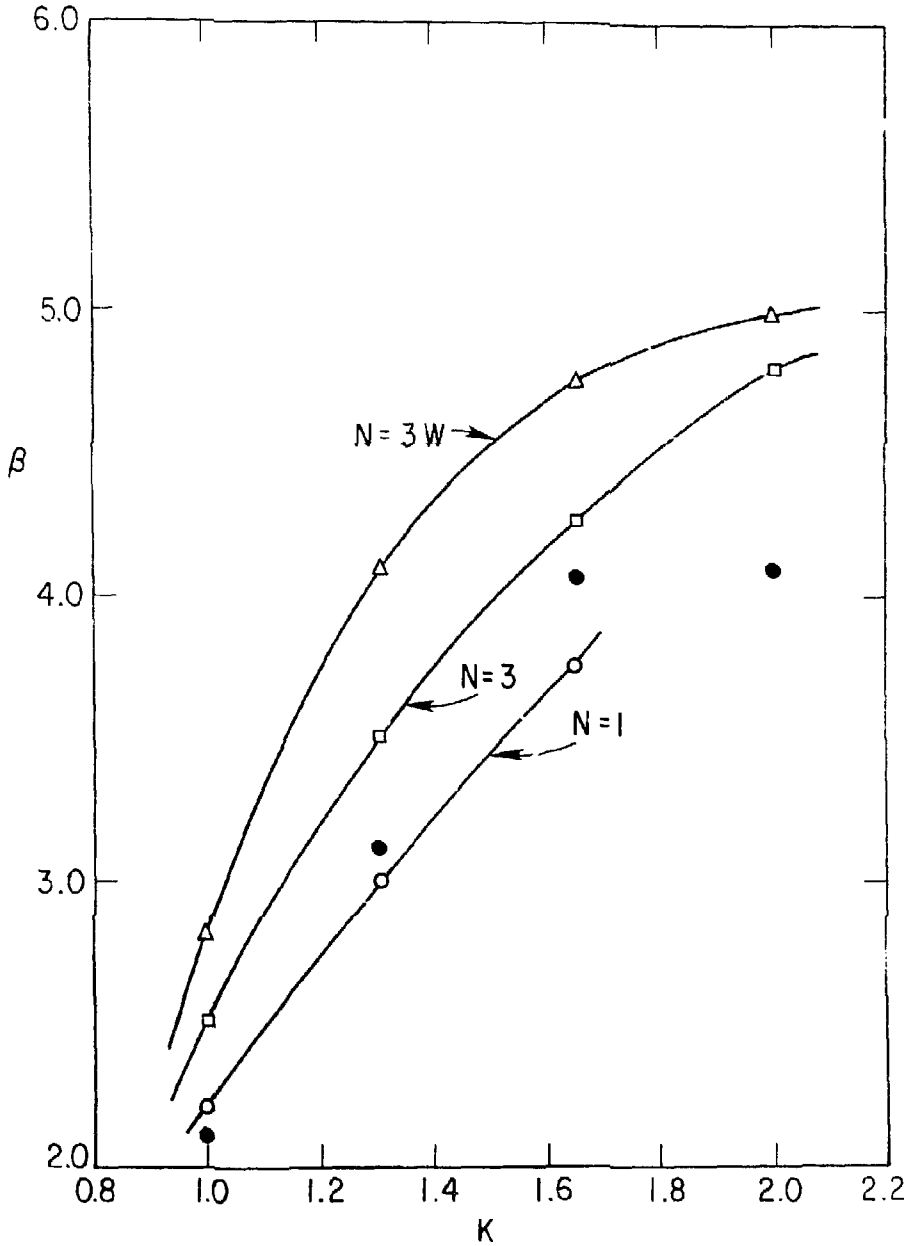

Fig. 4. 782244

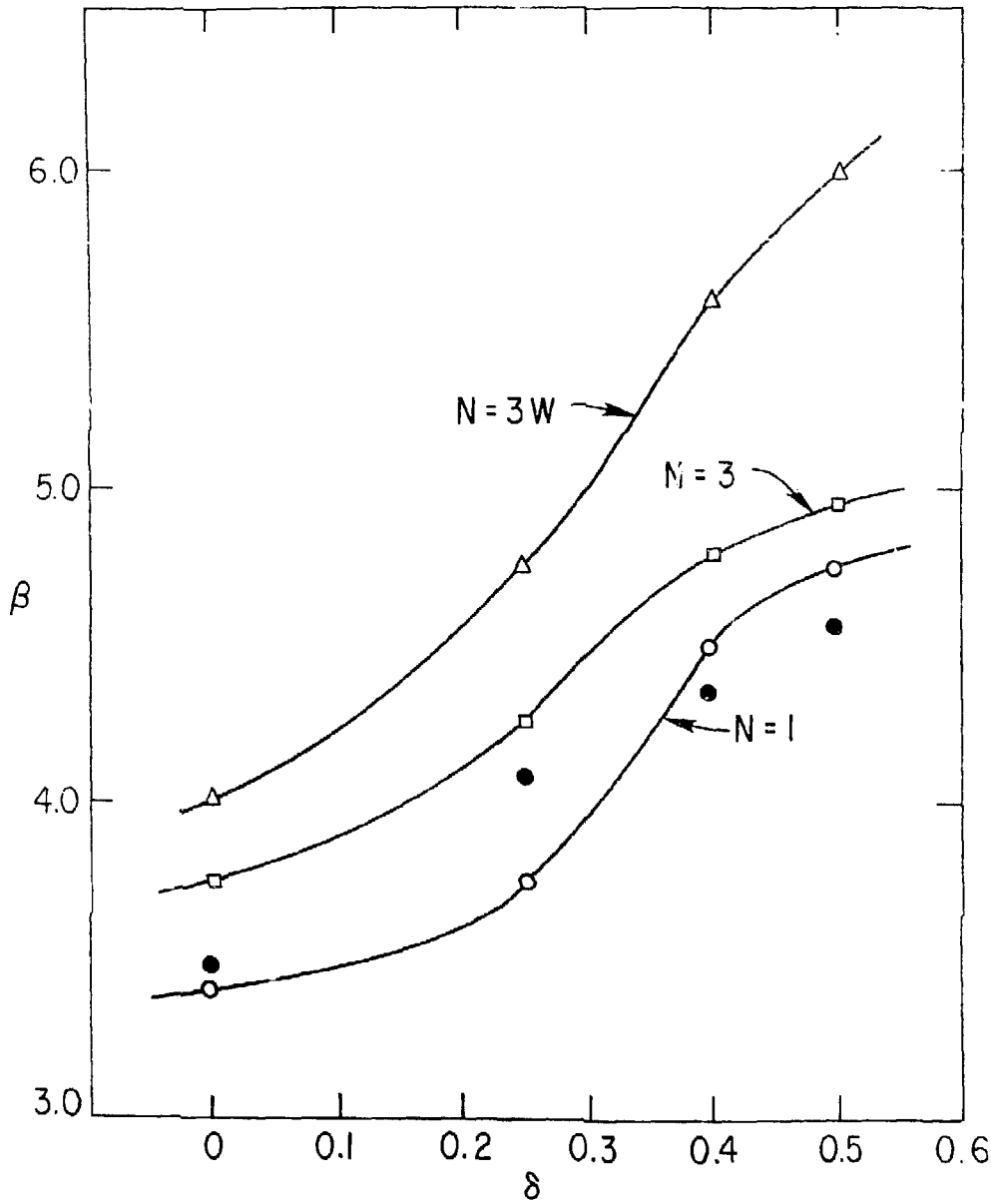

Fig. 5. 782245

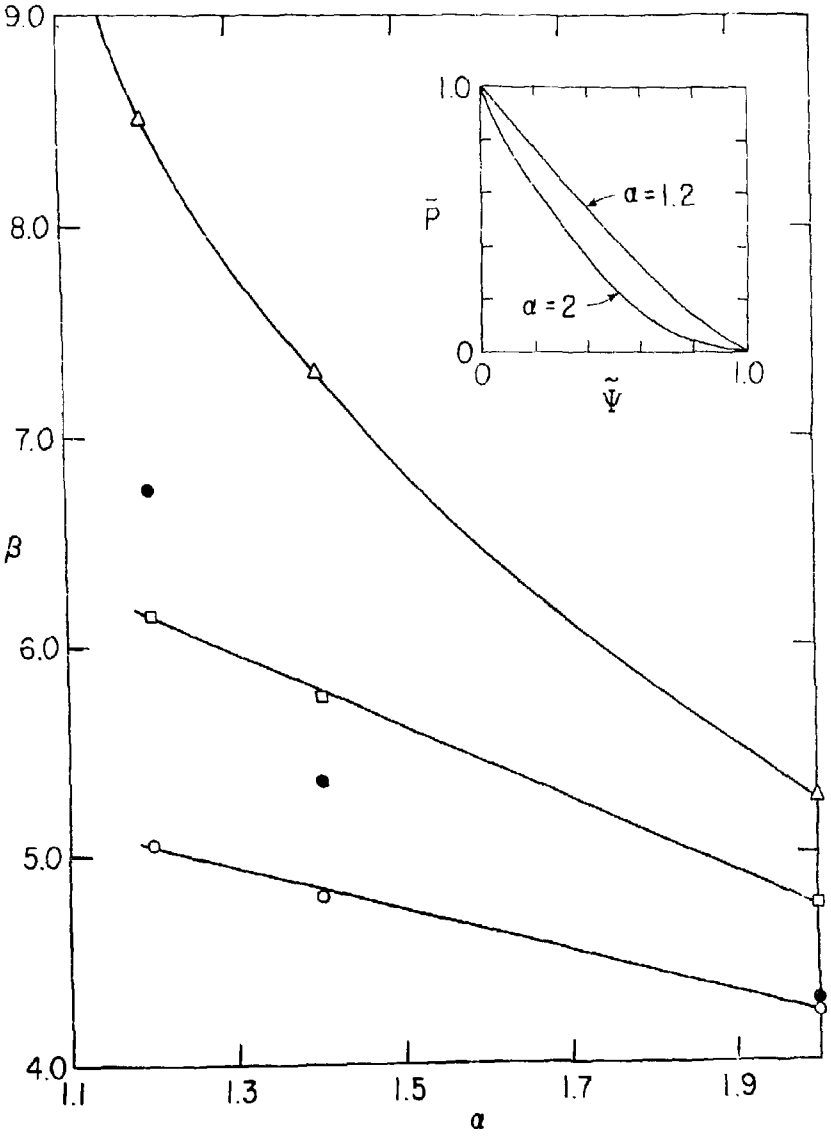

Fig. 6. 782249

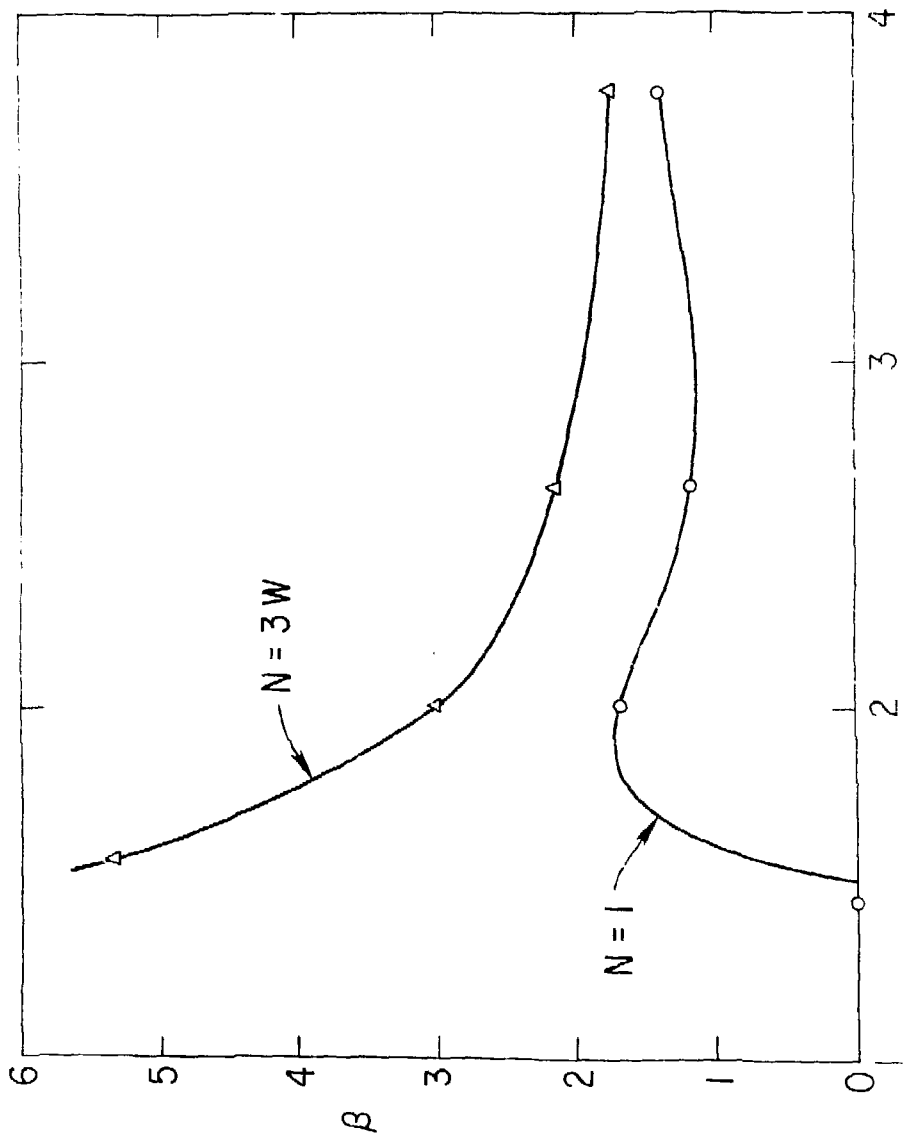

Fig. 7. 782243

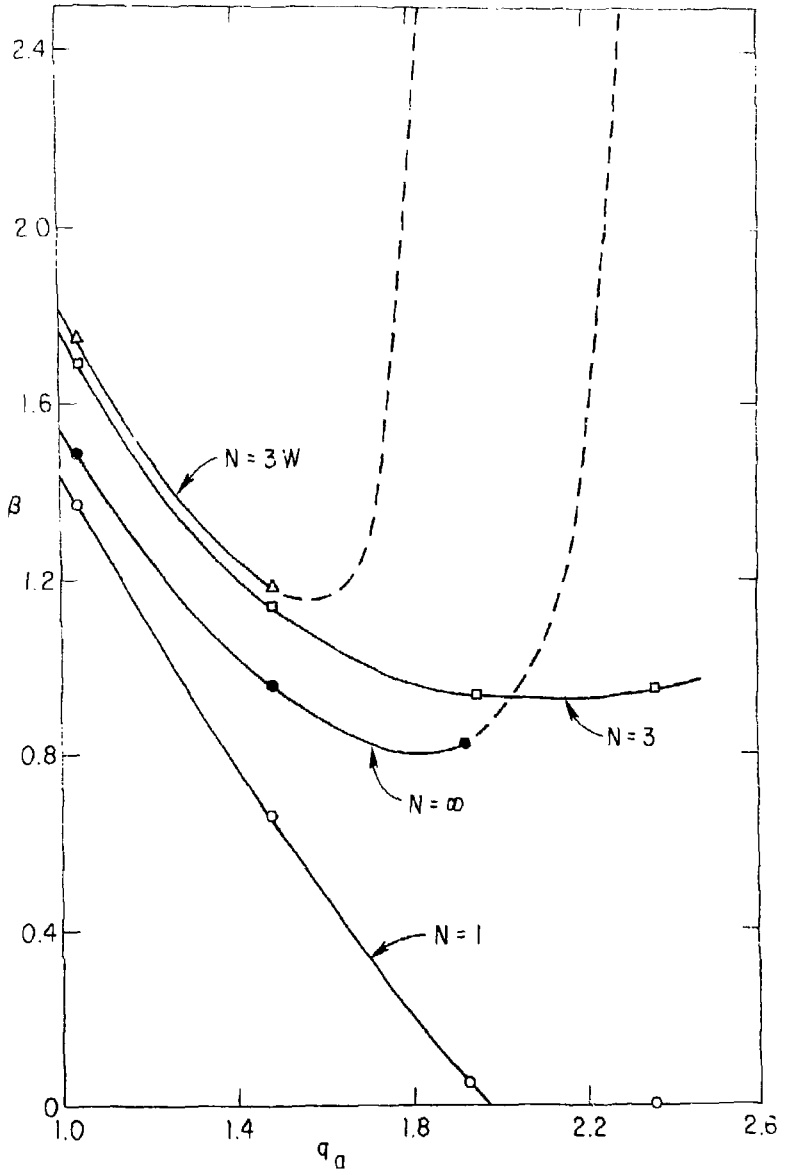

Fig. 8. 782246

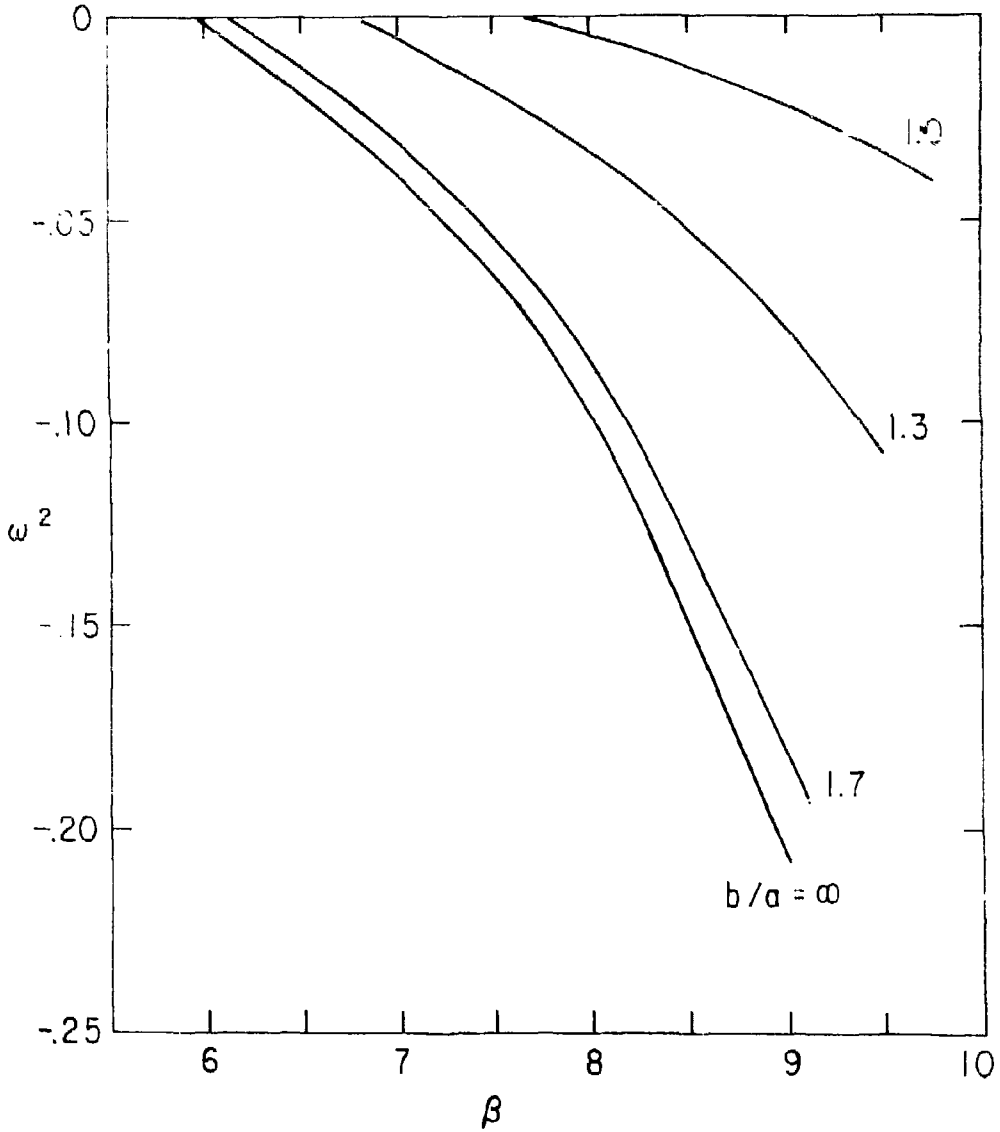

Fig. 9. 782231

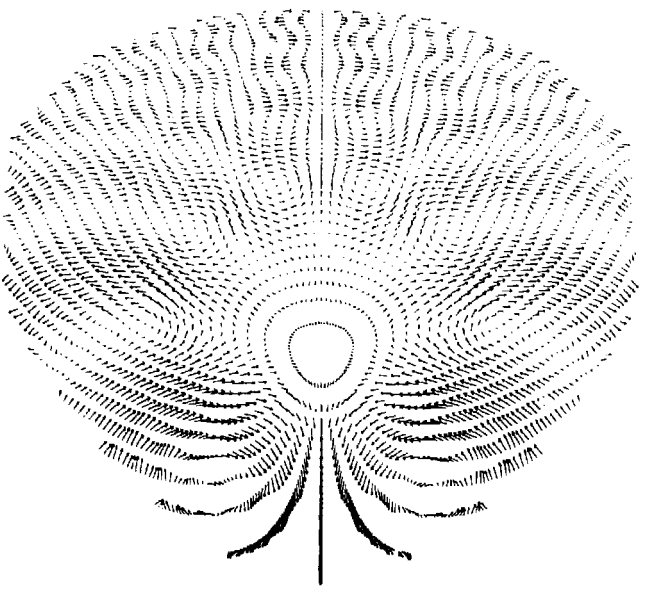

Fig. 10. 7°22.5'

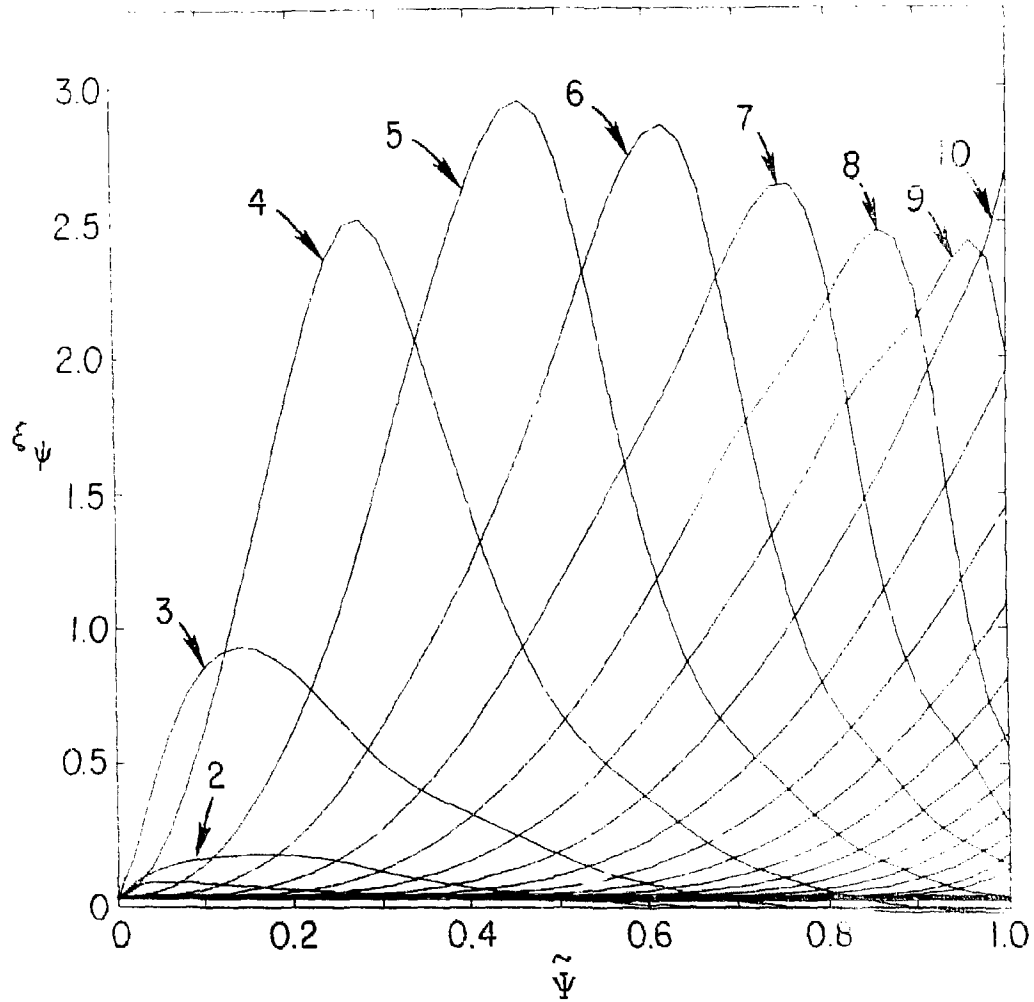

Fig. 11. 782240

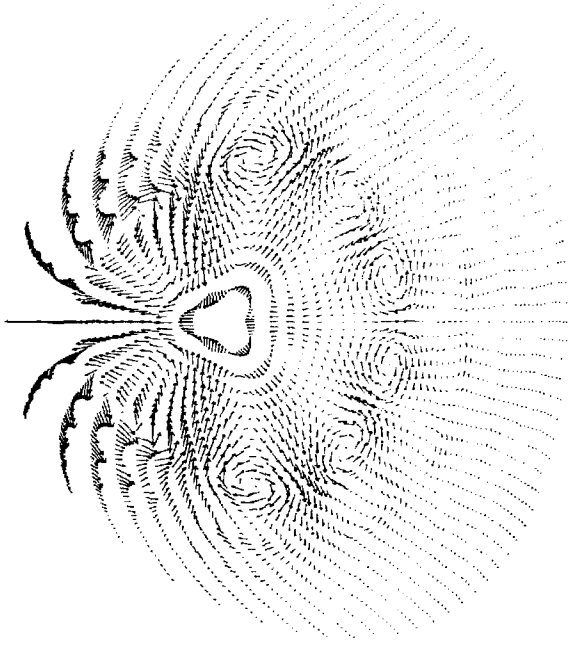

Fig. 13. 782235

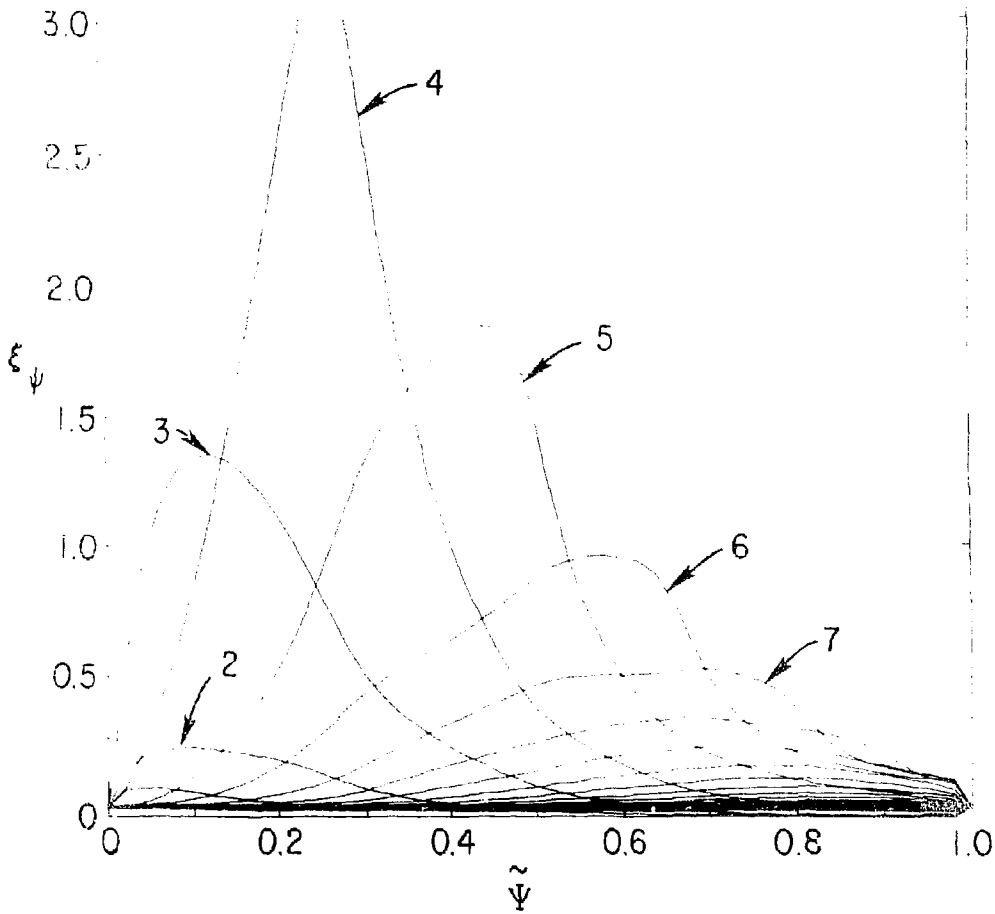

Fig. 13. 782239

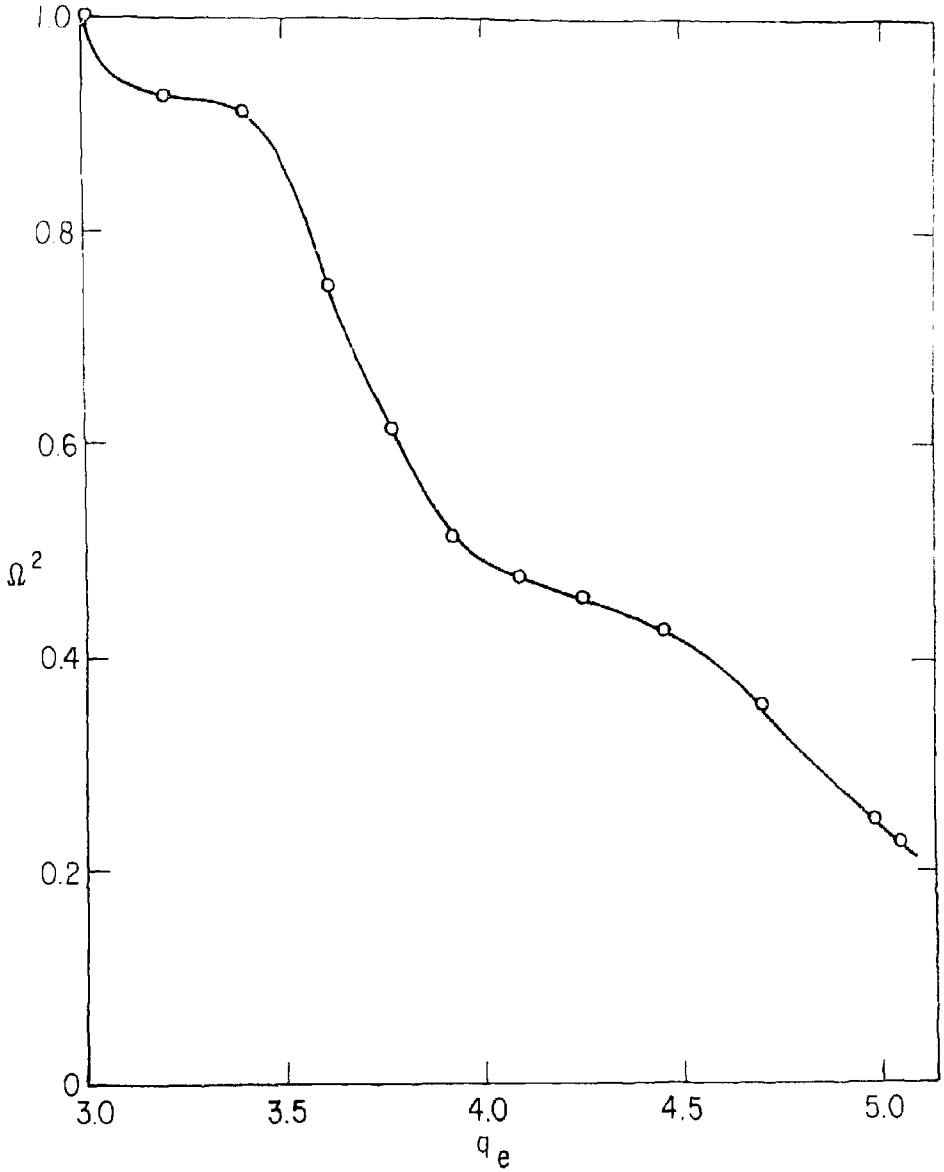

Fig. 14. 782248

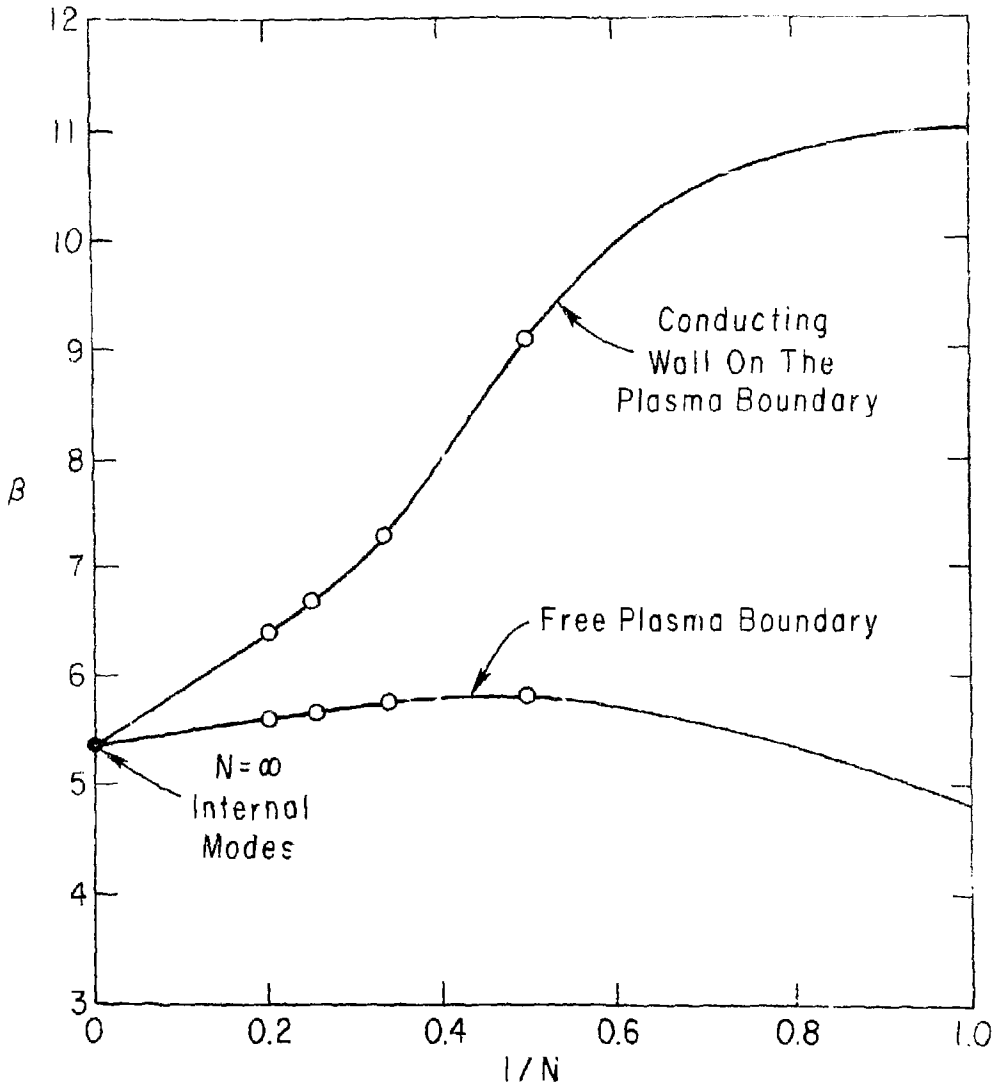

Fig. 15. 782226

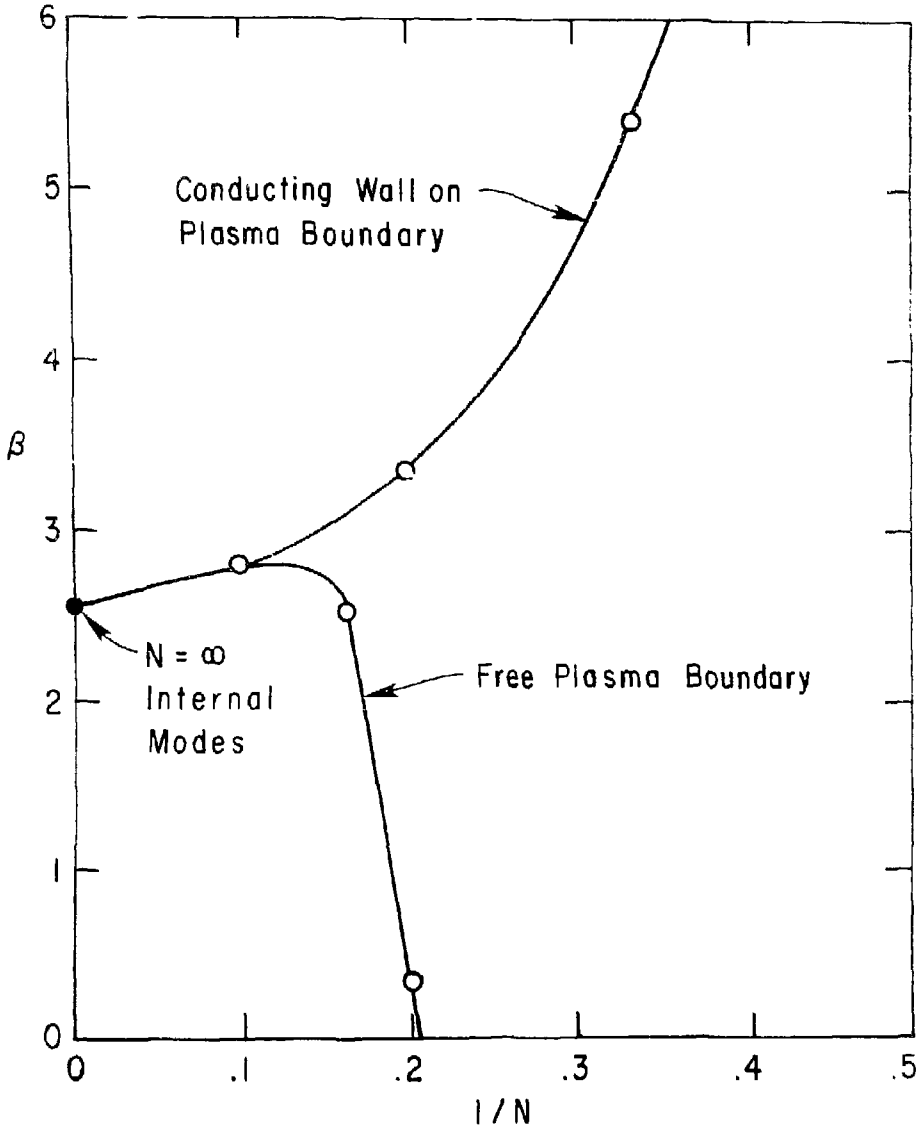

Fig. 16. 782241